bonding which, although asymmetric, shows a strong tendency toward development of a symmetric bond. The existence of a discrete hydrogen bond dimer rather than the more usual infinite spiral hydrogen bonded polymer observed for (X)(Y)PO(OH) compounds[12] is due to a steric effect as discussed previously.[5] The bulky *tert*-butyl groups in H[Dt-BP] are strategically located to block the directions in which a molecular approach is required to form a hydrogen-bonded spiral, while not interfering with dimer formation. Therefore dimeric hydrogen bonding is the only alternative.

The practical significance of the dimeric structure adopted by H[Dt-BP] is related to the obvious blockage of the oxygen chelation sites by the bulky *tert*-butyl groups, thus potentially interfering with extraction of metal ions of large ionic radii and high coordination number.[13] As reported in the Introduction, $R_2PO(OH)$ and $(RO)_2PO(OH)$ molecules, where R is a large organic ligand, extract $[UO2]^{2+}$ ions much more easily than ions of higher ionic radius and coordination number, e.g., Th(IV). Since the oxygen chelation sites are sterically blocked, ions of smaller radii can be expected to chelate more readily, e.g., the ionic radii of $[UO_2]^{2+}$ and Th(IV) are 0.76 Å (coordination no. 6) and 0.98 Å (coordination no. 8), respectively.

Clearly chelation of Th(IV) solely with H[Dt-BP] is not possible in view of the large radius and high charge and coordination number of Th(IV) plus the steric blockage of the oxygen sites of the extractant. Since Th(IV) is extracted to a minor extent by H[Dt-BP], water and inorganic anions probably participate somewhat to maintain the Th(IV) coordination sphere and charge balance.

Work is continuing on the synthesis and structural determinations of several metal–phosphorus chelated materials in order to pinpoint further the selective nature of many of these sterically hindered phosphinic acid extractants.

Registry No. H[Dt-BP], 677-76-9.

Supplementary Material Available: A listing of structure factor amplitudes (8 pages). Ordering information is given on any current masthead page.

References and Notes

(1) Work performed under the auspices of the U.S. Energy Research and Development Administration.
(2) To whom correspondence should be addressed.
(3) (a) D. F. Peppard, "Annual Review of Nuclear Science", Vol. 21, E. Segre, Ed., Annual Reviews Inc., Palo Alto, Calif., 1971, pp 365–396; (b) E. K. Hulet and D. D. Bode, *MTP Int. Rev. Sci.: Inorg. Chem., Ser. One*, 1 (1972); (c) G. W. Mason, N. L. Schofer, and D. F. Peppard, *J. Inorg. Nucl. Chem.*, **32**, 3899 (1970); (d) G. W. Mason, N. L. Schofer, and D. F. Peppard, *ibid.*, **32**, 3911 (1970); (e) D. F. Peppard, G. W. Mason, A. F. Bollmeier, and S. Lewey, *ibid.*, **33**, 845 (1971); (f) G. W. Mason and S. Lewey, *ibid*, **36**, 911 (1974).
(4) G. W. Mason and D. F. Peppard, unpublished results.
(5) M. E. Druyan, A. H. Reis, Jr., E. Gebert, S. W. Peterson, G. W. Mason, and D. F. Peppard, *J. Am. Chem. Soc.*, **98**, 4801 (1976).
(6) S. W. Peterson, R. P. Willett, and J. L. Huston, *J. Chem. Phys.*, **59**, 453 (1973).
(7) An IBM 370/195 program written by H. A. Levy.
(8) S5FOUR, S5XFLS, and S5FFE are Sigma 5 versions of the programs FOURIER by R. J. Dellaco and W. T. Robinson, ORXFLS3 written by W. R. Busing and H. A. Levy, and ORFFE3 written by W. R. Busing and H. A. Levy.
(9) "OR-TEP II" written by C. Johnson.
(10) W. Hamilton and J. Ibers, "Hydrogen Bonding in Solids", W. A. Benjamin, New York, N.Y., 1968, pp 53 and 54.
(11) C. H. Bushweller and J. A. Brunelle, *J. Am. Chem. Soc.*, **95**, 5949 (1973).
(12) (a) M. Calleri and J. C. Speakman, *Acta Crystallogr.*, **17**, 1097 (1964); (b) Mazhar-ul-Haque, C. N. Caughlan, and W. L. Moats, *J. Org. Chem.*, **35**, 1446 (1970); (c) F. P. Boer, *Acta Crystallogr., Sect. B*, **28**, 1201 (1972); (d) P. J. Wheatley, *J. Chem. Soc.*, **3722** (1962); (e) T.-T. Liang and K.-C. Chi, *Chem. Abstr.*, **63**, 12441e (1965); (f) F. Giordano and A. Ripamonti, *Acta Crystallogr.*, **22**, 678 (1967); (g) D. D. Swank and C. N. Coughlan, *Chem. Commun.*, 1051 (1968); (h) E. Alver and H. M. Kjoge, *Acta Chem. Scand.*, **23**, 1101 (1969); (i) D. Fenske, R. Mattes, J. Lons, and K. F. Tebbe, *Chem. Ber.*, **106**, 1139 (1973).
(13) The exact value for the size of an ion which will chelate has not been determined, but calculations based on extraction data seem to indicate that an ion with an ionic radius of ~0.80 Å or above will not fit satisfactorily.

Contribution from the Departments of Chemistry, State University of New York at Buffalo, Buffalo, New York 14214, and University of Illinois at Chicago Circle, Chicago, Illinois 60680

Molecules with an M_4X_4 Core. 8.[1–7] Crystal Structures of Tetrameric Triethylphosphinesilver(I) Chloride and Triethylphosphinesilver(I) Bromide

MELVYN ROWEN CHURCHILL,* JUDITH DONAHUE,[8] and FRANK J. ROTELLA

Received May 28, 1976 AIC60404+

The tetrameric species triethylphosphinesilver(I) chloride, $[PEt_3AgCl]_4$, and triethylphosphinesilver(I) bromide, $[PEt_3AgBr]_4$, have been synthesized and subjected to full three-dimensional x-ray structural analysis. The complexes each crystallize in the polar cubic space group $I\bar{4}3m$ (T_d^3; No. 217) with $Z = 2$. X-ray diffraction data were collected with a Picker FACS-1 automated diffractometer. Unit cell constants are $a = 12.919$ (2) Å for $[PEt_3AgCl]_4$ and $a = 13.165$ (2) Å for $[PEt_3AgBr]_4$. These species are isomorphous with $[PEt_3CuX]_4$ (X = Cl, Br, I) and $[AsEt_3CuI]_4$. However, satisfactory refinement of $[PEt_3AgCl]_4$ and $[PEt_3AgBr]_4$ occurred only after the additional assumption of threefold disorder of the silver atoms about the crystallographic C_3 axes. Resulting discrepancy indices are $R_F = 2.41\%$ and $R_{wF} = 2.49\%$ for $[PEt_3AgCl]_4$ and $R_F = 2.70\%$ and $R_{wF} = 2.52\%$ for $[PEt_3AgBr]_4$. Each molecule has a "cubanelike" skeleton of alternating silver and halogen atoms.

Introduction

We have recently completed crystal structure determinations on two complete series of tetrameric phosphinecopper(I) halides, $[PPh_3CuX]_4$ (X = Cl,[1] Br,[2] I[4]) and $[PEt_3CuX]_4$ (X = Cl,[5] Br,[5] I[3]), along with the related arsine derivative, $[AsEt_3CuI]_4$.[3] These results show the following pattern *for copper complexes*.

A. The ubiquitous "cubane" structure I is unstable with respect to the "step" structure II when large halogen atoms and bulky phosphine ligands appear simultaneously (i.e., in $[PPh_3CuI]_4$ and $[PPh_3CuBr]_4$); i.e., the transformation from "cubane" to "step" structure comes about as the result of repulsive intramolecular interactions. [Note that the step structure is not itself intrinsically unstable when intramolecular

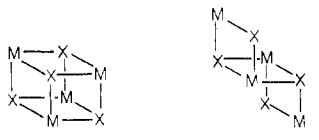

I II

* To whom correspondence should be addressed at the State University of New York at Buffalo.

repulsions are weak; rather, in this case, it can be viewed as a local potential minimum in the reaction coordinate for the formation of a cubane (M_4X_4) structure from the interaction of two dimers (M_2X_2) in solution. If the potential well is sufficiently deep, then the step structure will have an independent existence. It is thus not impossible that a step isomer of $[PPh_3CuCl]_4$ could exist; it is unlikely, however, that cubane isomers of $[PPh_3CuBr]_4$ or $[PPh_3CuI]_4$ will be obtained.]

B. All of the copper complexes $[ER_3CuX]_4$ (E = P or As, R = Ph or Et, X = Cl, Br, or I) which have been examined, whether they be cubane or step isomers, have intramolecular halogen···halogen distances which are indistinguishable from the sum of the appropriate van der Waals radii. Thus, the cubanelike cages of the $[PEt_3CuX]_4$ molecules are compressed such that their size is dictated by intramolecular halogen···halogen repulsions.

Phosphine–silver–halide complexes have been studied less extensively than their copper analogues. However, Churchill and DeBoer have reported a structural study of $[PEt_3AgI]_4$[7] (which has a cubane skeleton), while Teo and Calabrese have reported briefly on $[PPh_3AgCl]_4$ (cubane),[9] $[PPh_3AgBr]_4$ (cubane),[10] and $[PPh_3AgI]_4$ (both cubane and step isomers).[9] It is noteworthy that, as a result of the Ag^+ ion being larger than the Cu^+ ion, the silver–phosphine–halide species have structures in which the halogen···halogen distances are substantially greater than the sum of the appropriate van der Waals distances—i.e., the cage size is *not* dictated by intramolecular halogen···halogen repulsions.

The present work, consisting of structural studies on $[PEt_3AgCl]_4$ and $[PEt_3AgBr]_4$, was undertaken so that dimensions in an isoconnective set of $[PR_3AgX]_4$ complexes could be compared. However, as will be seen below, malignant Fate sat by and smiled.

Experimental Section

Synthesis of $[PEt_3AgCl]_4$ and $[PEt_3AgBr]_4$. 1. $[PEt_3AgCl]_4$. Approximately 3 ml of PEt_3 (2.4 g, 20 mmol) was injected into a slurry of AgCl (0.43 g, 3 mmol) in toluene (50 ml) under a positive pressure of nitrogen. The solution was stirred for 12 h at 90–100 °C and the solvent was then removed under reduced pressure. The product, a white powder with a trace of purple coloration (the latter due, presumably, to an impurity such as finely divided silver), was dissolved in hot toluene and filtered under suction and the residue was washed with a further aliquot of hot toluene. The volume of the solution was then reduced and the conical flask containing the solution was covered with Parafilm in which a small hole had been punched. After 2 days, transparent white crystals appeared, ranging in size from 1 to 125 mm^3. The crystals were filtered under suction, rinsed with CCl_4, and dried in the air; yield 0.30 g.

2. $[PEt_3AgBr]_4$. This material was prepared analogously to the preparation of $[PEt_3AgCl]_4$, starting with AgBr (3.0 g, 36 mmol) and PEt_3 (2.4 g, 20 mmol).

Collection of X-Ray Diffraction Data. 1. $[PEtAgCl]_4$. The crystal used was a characteristic rectangular dodecahedron (i.e., cubic with well-defined {110} faces). Perpendicular distances between parallel faces (or extensions thereof) were as follows, in mm: $(011) \rightarrow (0\bar{1}\bar{1}) = 0.049$, $(01\bar{1}) \rightarrow (0\bar{1}1) = 0.018$, $(101) \rightarrow (\bar{1}0\bar{1}) = 0.548$, $(10\bar{1}) \rightarrow (\bar{1}01) = 0.480$, $(110) \rightarrow (\bar{1}\bar{1}0) = 0.548$, $(1\bar{1}0) \rightarrow (\bar{1}10) = 0.484$. This crystal was wedged into a thin-walled glass capillary, which was then flushed with nitrogen, sealed, and mounted on a eucentric goniometer. Preliminary photographic data indicated that the crystal was cubic with O_h ($m3m$) symmetry. There are no systematic absences other than hkl for $h + k + l = 2n + 1$. Possible space groups are $I432$, $I\bar{4}3m$, and $Im3m$. The space group $I\bar{4}3m$ [T_d^3; No. 217] was selected because (i) it *requires* no disorder of the constituent $[PEt_3AgCl]_4$ molecules and (ii) it has been demonstrated to be the correct space group for the related species $[AsEt_3CuI]_4$,[3] $[PEt_3CuI]_4$,[3] $[PEt_3CuCl]_4$,[5] and $[PEt_3CuBr]_4$.[5]

The crystal was transferred to a Picker FACS-1 automated diffractometer, was accurately centered, and was aligned with [211] coincident with the ϕ axis. As a check on the severity of the absorption problem, the axial 422 reflection ($2\theta = 15.46°$) was measured, via θ–2θ scans, at $\chi = 90°$ and at 10° intervals from $\phi = 0°$ to $\phi = 350°$. The variation in intensity as a function of ϕ, defined by [(maximum − minimum)/average], was 48.1%; this was reduced to 5.3% upon application of an absorption correction. The crystal was now offset from its precise mounting along [211] so as to reduce the possible effects of multiple diffraction. Following redetermination of the orientation matrix and least-squares refinement of cell parameters and orientation parameters, data for one octant of the reciprocal sphere (i.e., *six* equivalent forms for general reflections) were collected. The experimental procedure has been described previously;[11] details specific to the present study are given in Table I.

2. $[PEt_3AgBr]_4$. A crystal of appropriate dimensions was cut from a much larger crystal. The resulting "lump" had no reentrant angles and was defined as a 14-sided polyhedron (a number of faces being of the type {110}) in which the maximum dimension was 0.38 mm. This crystal was aligned along (100), was found, photographically, to be isomorphous with the chloro compound, and was transferred to the diffractometer. The absorption problem was again examined by θ–2θ scans of an axial reflection (the 600, $2\theta = 18.6°$). The initial variation of 20.7% was reduced to 3.1% upon introduction of an absorption correction. Details of data collection are presented in Table I.

Solution and Refinement of Structure. 1. $[PEt_3AgCl]_4$. The following programs were used in the course of the structure determination: LSHF (structure factor calculations and full-matrix least-squares refinement, by B. G. DeBoer), FORDAP (Fourier synthesis, by A. Zalkin), STAN1 (calculation of distances and angles with esd's by B. G. DeBoer), and ORTEP (thermal ellipsoid drawings, by C. K. Johnson). All calculations were performed on the IBM 370/158 computer at the Computer Center of the University of Illinois at Chicago Circle.

Scattering factors for all atoms (neutral) except hydrogen were used in the analytical form of Cromer and Mann.[12] For hydrogen, the "best floated spherical H atom" values of Stewart et al.[13] were converted into analytical form.[14] The scattering factors of all nonhydrogen atoms were corrected for both the real and the imaginary components of anomalous dispersion, using the values of Cromer and Liberman.[15]

The function minimized during least-squares refinement was $\sum w[|F_o| - |F_c|]^2$ where the weight, w, is $[\sigma(F_o)]^{-2}$. The discrepancy indices, R_F and R_{wF}, are defined as

$$R_F = \left[\frac{\sum ||F_o| - |F_c||}{\sum |F_o|}\right] \times 100\ (\%)$$

$$R_{wF} = \left[\frac{\sum w(|F_o| - |F_c|)^2}{\sum w|F_o|^2}\right]^{1/2} \times 100\ (\%)$$

The "goodness of fit" is defined as

$$[\sum w(|F_o| - |F_c|)^2/(m - n)]^{1/2}$$

where m is the number of reflections and n is the number of variables.

Crystals of $[PEt_3AgCl]_4$ are isomorphous with those of the copper(I) analogue, $[PEt_3CuCl]_4$.[5] We therefore endeavored to solve the structure of the former starting from the known atomic coordinates of the latter. Exhaustive least-squares refinement (positional and anisotropic thermal parameters for all nonhydrogen atoms, coupled isotropic thermal parameters for methyl and methylene hydrogens with these atoms being fixed in an idealized staggered conformation, scale factor, and secondary extinction parameter), with atoms constrained precisely as in our previous study of $[PEt_3CuCl]_4$,[5] led to convergence with $R_F = 5.43\%$, $R_{wF} = 8.13\%$, and a "goodness of fit" of 4.530.

There were clear indications that this did not represent the "best possible" structural solution. These were as follows.

(1) The silver atom had alarmingly high thermal parameters—i.e., $B_{11} = B_{22} = B_{33} = 14.17\ (15)$ Å^2, $B_{12} = B_{13} = B_{23} = -4.92\ (7)$ Å^2, and $B_{equiv}(Ag) = 14.17$ Å^2. For comparison, the "equivalent isotropic thermal parameters" for metal atoms in related species are 5.68 Å^2 in $[AsEt_3CuI]_4$,[3] 5.98 Å^2 in $[PEt_3CuI]_4$,[3] 6.44 Å^2 in $[PEt_3CuBr]_4$,[5] 7.52 Å^2 in $[PEt_3CuCl]_4$,[5] and 8.31 Å^2 in $[PEt_3AgI]_4$.[7]

(2) The discrepancy indices, $R_F = 5.43\%$ and $R_{wF} = 8.13\%$, are far larger than expected. (The agreement between equivalent reflections in the sixfold averaging process, R_{F^2}, was 2.37% *based upon*

Table I. Experimental Data for X-Ray Diffraction Studies of $[PEt_3AgCl]_4$ and $[PEt_3AgBr]_4$

	$[PEt_3AgCl]_4$	$[PEt_3AgBr]_4$
	(A) Crystal Parameters	
Crystal system	Cubic	Cubic
Space group	$I\bar{4}3m$	$I\bar{4}3m$
a,[a] Å	12.9188 (22)	13.1651 (22)
V, Å^3	2156.1 (11)	2281.8 (11)
Temp, °C	19.0 (2)	20.6 (2)
Z	2	2
Mol wt	1045.933	1223.757
ρ(calcd), g cm^{-3}	1.611	1.781
ρ(obsd), g cm^{-3}	1.613 (5)[b]	1.768 (5)[b]
	(B) Measurement of Intensity Data[c]	
Radiation	Mo Kα	
Filters	Nb	
Attenuators	Cu foil; used if I(peak) > 10^4 counts/s	
Takeoff angle, deg	3.0	
Detector aperture, mm	6.3 × 6.3	
Crystal-detector distance mm	330	
Scan type	θ(crystal)-2θ(counter)	
Scan speed	1.0°/min	
Scan range	From $[2\theta(K\alpha_1) - 0.6]°$ to $[2\theta(K\alpha_2) + 0.6]°$	
Background measurement	20 s each at beginning and end of scan	
Crystal orientation (ϕ axis)	1.2° from [322]	14.3° from [100]
Reflections measd	$-h,+k,+l$	$+h,+k,+l$
Max 2θ, deg	50	45
Std reflections	3 after every 47	
Rms dev of standards[d,e]	$\bar{1}52$: 0.54%	310: 0.87%
	$\bar{5}21$: 0.52%	031: 1.06%
	$\bar{2}15$: 0.69%	103: 1.13%
Reflections collected[d]	1109	720
	(C) Reduction of Intensity Data	
Absorption coeff, cm^{-1}	21.85	52.98
Max and min transmission factors[f]	0.637–0.496	0.335–0.256
Symmetry-independent reflections	223	170
R_{F^2} for merging symmetry-related reflections[g]	2.37%	3.10%
Conversion to $\lvert F_o\rvert$ and $\sigma(\lvert F_o\rvert)$	As in ref 11	
"Ignorance factor"	0.025	0.040

[a] Unit cell parameters are derived from a least-squares fit to the setting angles of the Mo $K\alpha_1$ peaks (λ 0.709 30 Å) of 12 reflections ($2\theta \approx 39.4°$ for 12 forms of {5,5,10} for the chloro compound; $2\theta \approx 31$–$33°$ for 6 forms of {666} and 6 forms of {10,0,0} for the bromo compound). [b] Neutral buoyancy in aqueous BaI_2. [c] Unless otherwise stated, conditions for the data collection of the bromo compound paralleled those of the chloro compound. [d] The intensities of the standard reflections decreased slightly during the course of data collection (by about 2–3% for each compound). All data were corrected for this effect using a decay correction which was linear with time. [e] Data analysis and decay corrections were performed using the Fortran IV program **RDUS2**, by B. G. DeBoer. [f] Absorption corrections were applied using the program **DRABZ** by B. G. DeBoer. [g] $R_{F^2} = \Sigma\lvert F^2 - F_{av}^2\rvert/\Sigma\lvert F^2\rvert$ where F_{av}^2 is the average of the six (or three) independently measured symmetry-equivalent reflections. F^2 is the intensity of an individual reflection, and the sum is over all data averaged.

F^2! This corresponds to a random error of only 1.18% based upon F.) Structural studies on a series of isomorphous compounds had given far better results: R_F = 1.81%, R_{wF} = 1.73% vs. R_{F^2} = 1.98% for $[PEt_3CuBr]_4$;[5] R_F = 2.10%, R_{wF} = 2.41% vs. R_{F^2} = 2.23% for $[PEt_3CuCl]_4$[5]; R_F = 2.99%, R_{wF} = 3.36% vs. R_{F^2} = 2.05% for $[PEt_3AgI]_4$.[7] (We include no information on the species $[PEt_3CuI]_4$ and $[AsEt_3CuI]_4$[3] because hydrogen atom contributions were not incorporated into the structural solutions of these two molecules.)

(3) The "goodness of fit" value of 4.53 is, likewise, unreasonably high.

(4) A careful survey of the 223 reflections used in the structural study of $[PEt_3AgCl]_4$ showed that $\lvert F_o\rvert$ and $\lvert F_c\rvert$ disagreed by more than 10σ for 10 reflections and by 5σ–10σ for a further 31 reflections. (The most significant disagreements were $\lvert F_o\rvert - \lvert F_c\rvert = +15.5\sigma$ for 0,1,13 and -12.9σ for 3,3,10.)

We therefore computed a difference-Fourier synthesis. The most significant features were positive peaks of height 0.47 e Å^{-3} arranged like a trefoil about the crystallographic threefold [111] axis at positions (0.44, 0.38, 0.38), (0.38, 0.44, 0.38), and (0.38, 0.38, 0.44). Symmetrically disposed between these peaks were "troughs" of depth −0.60 e Å^{-3}. This pattern suggested that the silver atom did not lie on the axis at $x = y = z$ = 0.404 125 (11) (its refined position) but, rather, exhibited threefold disorder about the threefold axis [i.e., occupied the positions (x, x, z), (x, z, x), and (z, x, x), all of m symmetry].

This pattern of disorder was included in the model. Several cycles of full-matrix least-squares refinement led to the discrepancy indices being reduced from R_F = 28.92% and R_{wF} = 40.12% (the initial values with approximate silver positions and the old anisotropic thermal parameters) down to the final values of R_F = 2.41% and R_{wF} = 2.49% and to a final "goodness of fit" of 1.409. The largest shift during the final cycle of refinement was 0.001σ.

The final value for the secondary extinction parameter (c) was 1.93 (92) × 10^{-6} mm^{-1} e^{-2}. This parameter enters the equation for the corrected structure factor in the form[16–18]

$$F_{c,cor} = F_{c,uncor}(1 + c\beta F_{c,uncor}^2)^{-1/4}$$

where

$$\beta = \left(\frac{1 + \cos^4 2\theta}{(\sin 2\theta)(1 + \cos^2 2\theta)}\right)\left(\frac{-d \ln T}{d\mu}\right)$$

All features of the structural study were now satisfactory—the "equivalent isotropic thermal parameter" for the silver atom was now 8.629 Å^2, the largest disagreements between $\lvert F_o\rvert$ and $\lvert F_c\rvert$ were $+4.3\sigma$ for 0,3,11 and $+4.0\sigma$ for 0,8,12 (only two others were above 3σ), and the most significant features on a final difference-Fourier synthesis were peaks of height 0.23 e Å^{-3} [at (0.04, 0.04, 0.04)] and a trough of depth −0.12 e Å^{-3}.

Note that changing the structural model from one with ordered silver atoms to one with disordered silver atoms requires the addition of three parameters (we now have $x = y \neq z$, $B_{11} = B_{22} \neq B_{33}$, and $B_{12} \neq B_{13} = B_{23}$). With 223 observations and 28 parameters (the ordered model) we had R_{wF} = 8.13%; with 31 parameters (the disordered silver model), R_{wF} = 2.49%. The Hamilton R factor ratio

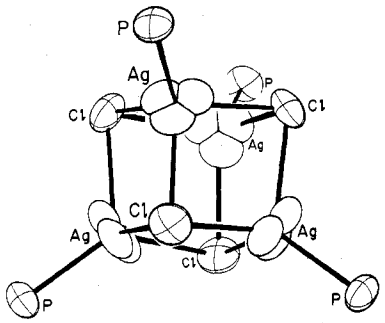

Figure 1. $P_4Ag_4Cl_4$ core of $[PEt_3AgCl]_4$, showing the threefold disorder of the silver atoms (ORTEP diagram, 30% probability ellipsoids).

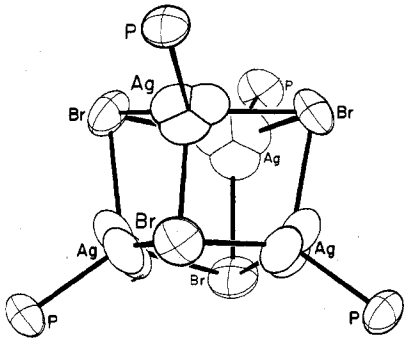

Figure 2. $P_4Ag_4Br_4$ core of $[PEt_3AgBr]_4$, showing the threefold disorder of the silver atoms.

test[19] indicates that for the disordered model to be preferred statistically over the ordered model at a 99.5% confidence level, its R_{wF} value must be lowered by a factor of approximately 1.04 ($\mathcal{R}_{b=3,n-m=120,\alpha=0.005}$ = 1.0547 and $\mathcal{R}_{b=3,n-m=250,\alpha=0.005}$ = 1.0269).[19] We have an observed R factor ratio of 3.27 which most assuredly represents a valid improvement!

As a final test of the handedness of the crystal investigated, we transformed all atomic coordinates x, y, z to $1-x, 1-y, 1-z$ and refined to convergence; resulting discrepancy indices were R_F = 2.89% and R_{wF} = 2.99%, and the "goodness of fit" was 1.689. Clearly the original choice of coordinates represented the correct enantiomorph; these latter results were rejected.

2. $[PEt_3AgBr]_4$. The crystallographic analysis of this species closely paralleled that of the chloro analogue (vide supra). The structure was solved by using the fractional coordinates for metal, phosphorus, and bromine atoms obtained from the isomorphous species $[PEt_3CuBr]_4$.[5] Subsequent introduction of carbon atoms and of hydrogen atoms in calculated positions and incorporation of a secondary extinction parameter led to convergence with R_F = 3.89%, R_{wF} = 3.54%, and a "goodness of fit" of 1.240. Despite these comfortably low values, there was some slight evidence that all was not well. The thermal parameters of the silver atom were huge ($B_{11} = B_{22} = B_{33}$ = 14.58 (10) Å^2, $B_{12} = B_{13} = B_{23}$ = −4.41 (6) Å^2, B_{equiv} = 14.58 Å^2). A difference-Fourier synthesis showed a pattern of threefold peaks and troughs about the ordered silver atom position [peak height 0.33 e Å^{-3} at (0.46, 0.39, 0.39), (0.39, 0.46, 0.39), (0.39, 0.39, 0.46); trough depths, radially between these peaks, −0.22 e Å^{-3}].

Continued refinement, now using disordered silver positions (as in the study of $[PEt_3AgCl]_4$) led to convergence with R_F = 2.70%, R_{wF} = 2.52%, and a "goodness of fit" of 0.891. The improvement in R_{wF} caused by the "disordering" of the silver atom is significant at a level of confidence far greater than 99.5%. (The observed R factor ratio with n = 170, m = 31, and b = 3 is 1.405; the tabulated value for $\mathcal{R}_{b=3,n-m=120,\alpha=0.005}$ is 1.0547.[19]).

The final value for the secondary extinction parameter was c = 1.26 (50) × 10^{-6} mm^{-1} e^{-2}.

A final difference-Fourier synthesis had, as its strongest feature, peaks of height 0.29 e Å^{-3} (at 0, 0, 0), 0.27 e Å^{-3} (at 0.46, 0.46, 0.46), and 0.25 e Å^{-3} (at 0.30, $^1/_2$, $^1/_2$).

The chirality of the crystal selected was tested by inverting all atomic coordinates from (x, y, z) to $(1-x, 1-y, 1-z)$. Refinement to convergence led to R_F = 4.60%, R_{wF} = 5.13%, and a "goodness of fit" of 1.814. Clearly the original choice of coordinates was correct.

A table of observed and calculated structure factor amplitudes is available as supplementary material. Final atomic positions are collected in Table II; anisotropic thermal parameters are listed in Table III.

Discussion

Interatomic distances for both $[PEt_3AgCl]_4$ and $[PEt_3AgBr]_4$ are given in Table IV. Selected bond angles are listed in Table V. The $P_4Ag_4X_4$ cores of these molecules are shown in Figures 1 and 2. Further views of these molecules (down one of their crystallographic S_4 axes) are presented in Figures 3 and 4.

The tetrameric $[PEt_3AgCl]_4$ and $[PEt_3AgBr]_4$ molecules each lie on sites of $\bar{4}3m$ (T_d) symmetry. The crystallographic asymmetric unit thus consists of $^1/_{24}$ of a molecule or $^1/_6$ of

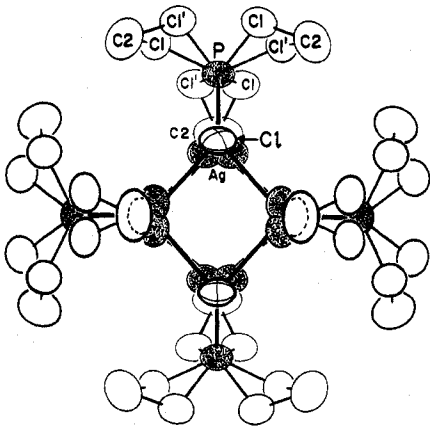

Figure 3. $[PEt_3AgCl]_4$ molecule viewed down an S_4 axis. Note disorder of the methylene carbon atoms (C(1) and C(1′)). Silver and phosphorus atoms are stippled. Hydrogen atoms are omitted for the sake of clarity.

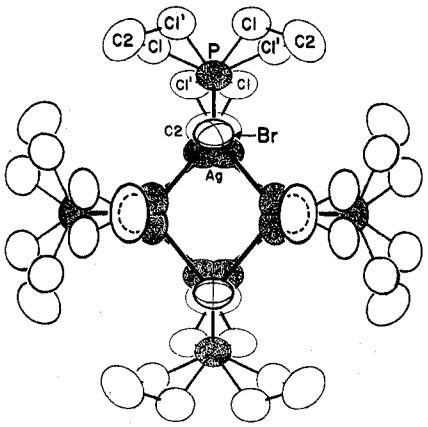

Figure 4. $[PEt_3AgBr]_4$ viewed down an S_4 axis; silver and phosphorus atoms are stippled.

a PEt_3AgX unit. While the $[PEt_3AgX]_4$ molecules could, in principle, be ordered (including even the hydrogen atoms), in practice this is not the case, and two patterns of disorder are observed.

(1) The ethyl groups are not bisected by the set of crystallographic $\{xxz\}$ mirror planes and are thus subject to disorder about these positions. Thus, the methylene carbon atom, the methylene hydrogen atoms, and the methyl hydrogen atoms are subject to a twofold disorder. [The terminal methyl carbon atoms appear to lie in the crystallographic mirror plane; however, it is not impossible that there are two unresolved sites for this atom related by the crystallographic mirror plane.] We note that this pattern of disorder is common to each of

Table II. Final Positional Parameters with Esd's[a]

Atom	Site symmetry	x	y	z	B,[b] Å^2
		A. $[(Et_3P)AgCl]_4$			
Ag[c]	m	0.392 22 (7)	=x	0.429 40 (10)	8.63
Cl	$3m$	0.607 45 (8)	=x	=x	8.76
P	$3m$	0.299 27 (7)	=x	=x	7.43
C(1)[d]	1	0.345 4 (7)	0.2819 (7)	0.168 2 (6)	9.40
C(2)	m	0.382 4 (5)	=x	0.118 9 (6)	14.39
H(1A)[d]	1	0.402 0	0.2351	0.169 0	13.3 (23)
H(1B)[d]	1	0.291 5	0.2544	0.126 4	
H(2A)[d]	1	0.422 8	0.4184	0.168 7	23.0 (40)
H(2B)[d]	1	0.323 7	0.4229	0.101 2	
H(2C)[d]	1	0.422 8	0.3702	0.058 8	
		B. $[(Et_3P)AgBr]_4$			
Ag[c]	m	0.397 10 (28)	=x	0.429 36 (52)	10.71
Br	$3m$	0.612 82 (7)	=x	=x	10.88
P	$3m$	0.303 63 (16)	=x	=x	9.64
C(1)[d]	1	0.350 4 (11)	0.2829 (11)	0.176 9 (11)	11.27
C(2)	m	0.381 3 (8)	=x	0.126 5 (10)	17.96
H(1A)[d]	1	0.406 9	0.2382	0.179 4	19.9 (62)
H(1B)[d]	1	0.297 9	0.2532	0.137 2	
H(2A)[d]	1	0.405 4	0.3686	0.059 7	17.8 (33)
H(2B)[d]	1	0.434 0	0.4113	0.165 7	
H(2C)[d]	1	0.325 0	0.4263	0.123 5	

[a] Esd's, shown in parentheses are right-adjusted to the last digit of the preceding number. They are derived from the inverse of the final least-squares matrix. [b] "Equivalent isotropic" thermal parameters are given for nonhydrogen atoms. For the full anisotropic thermal parameters, see Table III. [c] The silver atoms are subject to a threefold disorder about the C_3 axes (see text). [d] These atoms are disordered about the mirror plane at (x, x, z). See ref 3 and 5.

Table III. Anisotropic Thermal Parameters with Esd's[a,b]

Atom	B_{11}	B_{22}	B_{33}	B_{12}	B_{13}	B_{23}	$\langle U \rangle$[c]
			A. $[(Et_3P)AgCl]_4$				
Ag	8.79 (6)	=B_{11}	8.32 (10)	−3.31 (5)	−1.53 (4)	=B_{13}	0.23, 0.35, 0.39
Cl	8.76 (5)	=B_{11}	=B_{11}	−2.19 (4)	=B_{12}	=B_{12}	0.24, 0.37, 0.37
P	7.43 (5)	=B_{11}	=B_{11}	−1.54 (4)	=B_{12}	=B_{12}	0.23, 0.34, 0.34
C(1)	9.27 (45)	10.16 (44)	8.77 (39)	−2.46 (37)	0.45 (29)	−1.45 (30)	0.30, 0.33, 0.40
C(2)	16.04 (43)	=B_{11}	11.09 (45)	−5.92 (62)	1.55 (27)	=B_{13}	0.33, 0.40, 0.53
			B. $[(Et_3P)AgBr]_4$				
Ag	10.82 (22)	=B_{11}	10.48 (37)	−3.08 (14)	−2.14 (19)	=B_{13}	0.27, 0.40, 0.42
Br	10.88 (6)	=B_{11}	=B_{11}	−2.70 (4)	=B_{12}	=B_{12}	0.26, 0.41, 0.41
P	9.64 (10)	=B_{11}	=B_{11}	−1.94 (10)	=B_{12}	=B_{12}	0.27, 0.38, 0.38
C(1)	10.34 (89)	11.72 (89)	11.75 (88)	−3.49 (79)	−0.41 (64)	−1.85 (74)	0.30, 0.39, 0.44
C(2)	21.09 (91)	=B_{11}	11.72 (77)	−8.5 (13)	−0.22 (56)	=B_{13}	0.38, 0.40, 0.61

[a] See footnote *a* to Table II. [b] These anisotropic thermal parameters are analogous to the usual form of the isotropic thermal parameter and have units of Å^2. They enter the expression for the calculated structure-factor amplitude in the form $\exp[-0.25a^{*2}(h^2B_{11} + k^2B_{22} + l^2B_{33} + 2hkB_{12} + 2hlB_{12} + 2klB_{23})]$. [c] These values are the root-mean-square amplitudes of vibration (in Å) of the atom along the three principal axes (minor, median, major, respectively) of its vibrational ellipsoid. For relative orientations, see the figures.

the previously studied isomorphous species—$[AsEt_3CuI]_4$,[3] $[PEt_3CuI]_4$,[3] $[PEt_3CuCl]_4$,[5] and $[PEt_3CuBr]_4$;[5] it is also found in *tetragonal* $[PEt_3AgI]_4$.[7]

(2) In addition, the silver atoms are subject to a threefold disorder (vide infra) about the crystallographic C_3 axes. The degree of disorder is such that Ag(x, x, z)···Ag(x, z, x) = Ag(x, z, x)···Ag(z, x, x) = Ag(z, x, x)···Ag(x, x, z) = 0.6793 (25) Å for $[PEt_3AgCl]_4$ and 0.6007 (141) Å for $[PEt_3AgBr]_4$. The silver atoms are displaced from the crystallographic C_3 axes by 0.3922 and 0.3468 Å for the chloro and bromo compound, respectively.

The observed threefold disorder of the silver atoms can be explained by either of the following: (A) the silver atoms are not truly disordered but undergo large vibrational motions such that the volume swept out more closely resembles a trefoil than an ellipsoid; (B) the crystal is composed of $[PEt_3AgX]_4$ molecules disordered in some way such that there is threefold disorder of the silver atoms but essential coincidence of all other atoms.

Possibility B seems to be the most likely. In this case the individual $[PEt_3AgCl]_4$ and $[PEt_3AgBr]_4$ molecules must have $P_4Ag_4X_4$ cores in which the molecular symmetry is reduced from T_d. Since we observe threefold disorder of the silver atoms, the true point group of the $P_4Ag_4X_4$ (X = Cl, Br) cores is D_{2d} or some subgroup thereof (i.e., T_d with at least all C_3 axes and concomitant symmetry elements removed). Interestingly, the related molecular species $[PEt_3AgI]_4$, which crystallizes in the tetragonal system, has precise D_{2d} symmetry.

Within the disordered arrays which constitute the $[PEt_3AgCl]_4$ and $[PEt_3AgBr]_4$ structures (see Figures 1 and 2) there is but a single independent Ag–P bond length and a single independent X···X contact. The three Ag–X distances, while not all equivalent, are uniquely determined. The sole major problem in interpreting the intramolecular vectors comes in determining which of the Ag···Ag distances (see Table IV) belong to a given molecule and which represent vectors between overlapping molecular images. This problem can be elucidated via the following considerations.

(i) The disordered $[PEt_3AgX]_4$ molecules each contain 12 sites for silver atoms.

(ii) Each $P_4Ag_4X_4$ cluster is assumed to retain at least an S_4 axis, the maximum possible molecular symmetry being D_{2d}.

(iii) The vectors of length 0.6793 (25) Å (for X = Cl) and 0.6007 (141) Å (for X = Br) are clearly between molecules

Table IV. Intramolecular Distances (Å) with Esd's[a]

Atoms	$[PEt_3AgCl]_4$	$[PEt_3AgBr]_4$
Ag···Ag (z, x, x)	0.6793 (25)	0.6007 (141)
Ag···Ag (x, z, x)	0.6793 (25)	0.6007 (141)
Ag···Ag ($1-z, x, 1-x$)	3.2590 (20)	3.2310 (62)
Ag···Ag ($x, 1-z, 1-x$)	3.2590 (20)	3.2310 (62)
Ag···Ag ($x, 1-x, 1-z$)	3.3291 (19)	3.2863 (45)
Ag···Ag ($1-x, x, 1-z$)	3.3291 (19)	3.2863 (45)
Ag···Ag ($1-x, 1-z, x$)	3.6465 (22)	3.5695 (58)
Ag···Ag ($1-z, 1-x, x$)	3.6465 (22)	3.5695 (58)
Ag···Ag ($z, 1-x, 1-x$)	3.6465 (22)	3.5695 (58)
Ag···Ag ($1-x, z, 1-x$)	3.6465 (22)	3.5695 (58)
Ag···Ag ($1-x, 1-x, z$)	3.9384 (28)	3.8317 (103)
Ag-P	2.3895 (20)	2.4018 (48)
Ag-X ($1-x, 1-x, x$)	2.3002 (17)	2.4222 (71)
Ag-X ($1-x, x, x$)	2.8211 (15)	2.8967 (46)
Ag-X ($x, 1-x, 1-x$)	2.8211 (15)	2.8967 (46)
Ag···X (x, x, x)	4.5557 (21)	4.6866 (25)
X···X	3.9263 (31)	4.2009 (27)
P-C(1)	1.809 (7)	1.799 (13)
C(1)-C(2)	1.523 (12)	1.512 (17)
C(1)···C(1′)	1.159 (20)	1.256 (32)

[a] Esd's, shown in parentheses, are right-adjusted to the last digit of the preceding number. These calculations, carried out using the Fortran IV program STAN 1 (by Dr. B. G. DeBoer), include the effects of the full positional covariance matrix and the uncertainties in the unit cell parameters. No corrections have been made for the possible effects of thermal motion.

Table V. Selected[a] Bond Angles (deg) with Esd's[b]

Atoms	$[PEt_3AgCl]_4$	$[PEt_3AgBr]_4$
X[$x, 1-x, 1-x$]-Ag-X[$1-x, x, 1-x$]	88.20 (6)	92.96 (19)
X[$x, 1-x, 1-x$]-Ag-X[$1-x, 1-x, x$]	99.61 (6)	103.98 (10)
X[$1-x, x, 1-x$]-Ag-X[$1-x, 1-x, x$]	99.61 (6)	103.98 (10)
P-Ag-X[$x, 1-x, 1-x$]	112.17 (5)	110.31 (19)
P-Ag-X[$1-x, x, 1-x$]	112.17 (5)	110.31 (19)
P-Ag-X[$1-x, 1-x, x$]	134.86 (8)	129.20 (30)
Ag[$x, 1-x, 1-z$]-X-Ag[$1-x, 1-z, x$]	80.53 (6)	76.07 (9)
Ag[$x, 1-x, 1-z$]-X-Ag[$1-x, z, 1-x$]	90.21 (8)	83.79 (18)
Ag[$1-x, 1-z, x$]-X-Ag[$1-x, z, 1-x$]	80.39 (6)	75.73 (10)
Ag-P-C(1)	123.74 (28)	122.78 (45)
Ag-P-C(1)[z, x, y]	113.09 (26)	113.84 (41)
Ag-P-C(1)[y, z, x]	107.53 (27)	108.48 (45)
C(1)-P-C(1)[z, x, y]	103.47 (32)	103.22 (49)
C(1)-P-C(1)[y, z, x]	103.47 (32)	103.22 (49)
C(1)[y, z, x]-P-C(1)[z, x, y]	103.47 (32)	103.22 (49)
P-C(1)-C(2)	112.87 (56)	111.70 (95)

[a] All angles refer to the molecule generated via an $S_4(x)$ operation involving the silver atom at x, x, z (see text). [b] See footnote *a* to Table IV.

in alternative sites. We can also predict that the longest and shortest of the remaining Ag···Ag vectors will be between overlapping molecular images and will not represent true intramolecular distances.

(iv) The basic silver atom at x, x, z could be associated with any of three possible molecular images, corresponding to possible real molecules having true S_4 ($\bar{4}$) axes lying along x, y, and z (respectively).

(v) We will now consider those possible ordered arrangements of silver atoms which include that at x, x, z, with a view toward determining which images have a "sensible" molecular geometry. The possible quartets of silver atoms thus generated are shown in Chart I.

Chart I. Ag Coordinates

S_4 along x ($S_4(x)$)
x, x, z
$1-x, 1-z, x$
$x, 1-x, 1-z$
$1-x, z, 1-x$

S_4 along y ($S_4(y)$)
x, x, z
$1-z, 1-x, x$
$1-x, x, 1-z$
$z, 1-x, 1-x$

S_4 along z ($S_4(z)$)
x, x, z
$1-x, x, 1-z$
$1-x, 1-x, z$
$x, 1-x, 1-z$

Table VI. Comparison of Interatomic Distances (Å) for the Cubanelike Series $[PEt_3CuX]_4$, $[PEt_3AgX]_4$, and $[PPh_3AgX]_4$

Molecule	$[PEt_3CuCl]_4$[a]	$[PEt_3CuBr]_4$[a]	$[PEt_3CuI]_4$[b]
Cu···Cu	3.2111 (16)	3.1836 (18)	2.9272 (20)
X···X	3.6567 (22)	3.9324 (13)	4.3800 (11)
Cu-X	2.4383 (10)	2.5436 (08)	2.6837 (13)
Cu-P	2.1757 (17)	2.1994 (22)	2.2538 (27)
Molecule	$[PEt_3AgCl]_4$	$[PEt_3AgBr]_4$	$[PEt_3AgI]_4$[c]
Ag···Ag	3.5407 (estd)[f]	3.4751 (estd)[f]	3.2083 (av)
X···X	3.9263 (31)	4.2009 (27)	4.7527 (av)
Ag-X	2.6475 (av)	2.7385 (av)	2.9187 (av)
Ag-P	2.3895 (20)	2.4018 (48)	2.4379 (19)
Molecule	$[PPh_3AgCl]_4$[d]	$[PPh_3AgBr]_4$[e]	$[PPh_3AgI]_4$[d]
Ag···Ag	3.633 (av)	3.825 (av)	3.483 (av)
X···X	3.838 (av)	4.082 (av)	4.583 (av)
Ag-X	2.654 (av)	2.800 (av)	2.911 (av)
Ag-P	2.379 (av)	2.422 (av)	2.461 (av)

[a] See ref 5. [b] See ref 3. [c] See ref 7. [d] See ref 9. [e] See ref 10. [f] See text.

We can determine which of the three S_4 axes will generate a $[PEt_3AgX]_4$ molecule of acceptable geometry *starting with the silver atom at x, x, z.*

For $[PEt_3AgCl]_4$, the $S_4(x)$ axis generates a tetrahedral Ag_4 grouping in which the Ag···Ag vectors are of length 3.3291 Å (two times) and 3.6465 Å (four times); the $S_4(y)$ axis similarly generates a system with Ag···Ag vectors of 3.3291 Å (two times) and 3.6465 Å (four times); the $S_4(z)$ axis generates Ag···Ag vectors of length 3.3291 Å (four times) and 3.9384 Å (two times). The geometry of this last system is too distorted and is eliminated. Ag(x, x, z) therefore generates acceptable tetrahedral Ag_4 systems either via an $S_4(x)$ or an $S_4(y)$ axis. It can be shown that the other two silver sites near Ag(x, x, z) behave in a related manner. Thus, Ag(x, z, x) generates molecules of acceptable geometry via the rotation–reflection axes $S_4(x)$ or $S_4(z)$ and Ag(z, x, x) generates acceptable molecules via $S_4(y)$ or $S_4(z)$ operations.

The Ag_4 system in $[PEt_3AgCl]_4$ is thus an elongated tetrahedron in which two Ag···Ag vectors are 3.3291 (19) Å and the other four Ag···Ag vectors are 3.6465 (22) Å (average 3.5407 Å). Corresponding distances for $[PEt_3AgBr]_4$, using identical arguments, are 3.2863 (45) Å (two times) and 3.5695 (58) Å (four times), with an average Ag···Ag distance of 3.4751 Å.

The interatomic distances of $[PEt_3AgCl]_4$ and $[PEt_3AgBr]_4$ are compared with the known parameters of $[PEt_3AgI]_4$ in Table VI; data on the known cubanelike series $[PEt_3CuX]_4$ and $[PPh_3AgX]_4$ (X = Cl, Br, I) are also included in this compilation.

We note the following systematic effects on interatomic distances within the $[PEt_3AgX]_4$ (X = Cl, Br, I) molecules.

(1) Silver–halogen distances increase systematically with increasing mass of the halogen atom. Thus, Ag–Cl = 2.6475 Å, Ag–Br = 2.7385 Å, and Ag–I = 2.9187 Å. The successive increments of 0.0910 and 0.1802 Å closely resemble those found within the analogous copper(I) species, $[PEt_3CuX]_4$ (increments are 0.1053 and 0.1401 Å).[5]

(2) Intramolecular halogen···halogen distances increase smoothly within the $[PEt_3AgX]_4$ (X = Cl, Br, I) series, with Cl···Cl in $[PEt_3AgCl]_4$ being 3.9263 Å, Br···Br in $[PEt_3AgBr]_4$ being 4.2009 Å, and I···I in $[PEt_3AgI]_4$ being 4.7527 Å. The incremental changes of 0.2746 and 0.5518 Å are fairly close to those found in the $[PEt_3CuX]_4$ series (0.2757 and 0.4476 Å). However, it must be emphasized strongly that the halogen···halogen distances within the $[PEt_3CuX]_4$ molecules are all at approximately the distance dictated by the van der Waals repulsive forces and therefore are important in dictating the molecular geometry—at least insofar as they determine the minimum size that the Cu_4X_4 cluster can have. The X···X distances within the $[PEt_3AgX]_4$ molecules are all significantly greater than the sum of the van der Waals radii.[20] [Cl···Cl(obsd) = 3.9263 Å vs. Cl···Cl(van der Waals) = 3.6 Å; Br···Br(obsd) = 4.2009 Å vs. 3.9 Å; I···I(obsd) = 4.7527 Å vs. 4.3 Å].

(3) Silver···silver distances within the $[PEt_3AgX]_4$ molecules *decrease* with increasing size of halogen atom, individual values being 3.5407 Å in $[PEt_3AgCl]_4$, 3.4751 Å in $[PEt_3AgBr]_4$, and 3.2083 Å in $[PEt_3AgI]_4$. The successive decrements of 0.0656 and 0.2668 Å again closely resemble those in the $[PEt_3CuX]_4$ series (0.0275 and 0.2564 Å, respectively).

(4) Silver–phosphorus distances increase systematically with values of 2.3895 (20) Å in $[PEt_3AgCl]_4$, 2.4018 (48) Å in $[PEt_3AgBr]_4$, and 2.4379 (19) Å in $[PEt_3AgI]_4$. Similar trends are found in both the $[PEt_3CuX]_4$ and the $[PPh_3AgX]_4$ series and are believed to result from decreased Cu → P back-donation as the electronegativity of X decreases.[5]

Acknowledgment. This work was generously supported by the National Science Foundation through Grant No. CHE76-05564 to M.R.C.

Registry No. $[PEt_3AgCl]_4$, 60349-53-3; $[PEt_3AgBr]_4$, 60349-54-4.

Supplementary Material Available: Listing of structure factor amplitudes (1 page). Ordering information is given on any current masthead page.

References and Notes

(1) Part 1: M. R. Churchill and K. L. Kalra, *Inorg. Chem.*, **13**, 1065 (1974).
(2) Part 2: M. R. Churchill and K. L. Kalra, *Inorg. Chem.*, **13**, 1427 (1974).
(3) Part 3: M. R. Churchill and K. L. Kalra, *Inorg. Chem.*, **13**, 1899 (1974).
(4) Part 4: M. R. Churchill, B. G. DeBoer, and D. J. Donovan, *Inorg. Chem.*, **14**, 617 (1975).
(5) Part 5: M. R. Churchill, B. G. DeBoer, and S. J. Mendak, *Inorg. Chem.*, **14**, 2041 (1975).
(6) Part 6: M. R. Churchill, B. G. DeBoer, and S. J. Mendak, *Inorg. Chem.*, **14**, 2496 (1975).
(7) Part 7: M. R. Churchill and B. G. DeBoer, *Inorg. Chem.*, **14**, 2502 (1975).
(8) Undergraduate Student participant at U.I.C.C., Spring 1975.
(9) B. K. Teo and J. C. Calabrese, *J. Am. Chem. Soc.*, **97**, 1256 (1975).
(10) B. K. Teo and J. C. Calabrese, *J. Chem. Soc., Chem. Commun.*, 185 (1976).
(11) M. R. Churchill and B. G. DeBoer, *Inorg. Chem.*, **12**, 525 (1973).
(12) D. T. Cromer and J. B. Mann, *Acta Crystallogr., Sect. A*, **24**, 321 (1968).
(13) R. F. Stewart, E. R. Davidson, and W. T. Simpson, *J. Chem. Phys.*, **42**, 3175 (1965).
(14) See ref 4, footnote 14.
(15) D. T. Cromer and D. Liberman, *J. Chem. Phys.*, **53**, 1891 (1970).
(16) W. H. Zachariasen, *Acta Crystallogr.*, **16**, 1139 (1963); **23**, 558 (1967).
(17) A. C. Larson in "Crystallographic Computing", F. R. Ahmed, Ed., Munksgaard, Copenhagen, 1970, p 29 ff.
(18) Note that $-d \ln T/d\mu = \bar{t}$, the weighted average path length (in mm) of x rays through the crystal.
(19) "International Tables for X-Ray Crystallography", Vol. 4, Kynoch Press, Birmingham, England, 1974; see Table 4.2, pp 288–292.
(20) L. Pauling, "The Nature of the Chemical Bond", 3d ed, Cornell University Press, Ithaca, N.Y., 1960, p 260.

Contribution No. 5343 from the Arthur Amos Noyes Laboratory of Chemical Physics, California Institute of Technology, Pasadena, California 91125

Preparation and Structural Characterization of a Monomeric Dioxygen Adduct of (*N*,*N*′-(1,1,2,2-Tetramethylethylene)bis(salicylideniminato))(1-benzylimidazole)cobalt(II)

ROBERT S. GALL and WILLIAM P. SCHAEFER*

Received June 2, 1976 AIC604106

The synthesis and structural characterization of a monomeric σ-bonded dioxygen adduct of (*N*,*N*′-(1,1,2,2-tetramethylethylene)bis(salicylideniminato))cobalt(II) with 1-benzylimidazole as the axial base, Co(saltmen)(BzlImid)(O_2), are reported. The dioxygen adduct crystallizes as a tetrahydrofuran solvate at −18 °C. The crystals are monoclinic (space group $P2_1/c$) with a = 11.485 (1) Å, b = 14.566 (1) Å, c = 19.102 (1) Å, β = 93.596 (5)°, and Z = 4. The calculated density is 1.340 g cm^{-3}. Anisotropic least-squares refinement gave R = 0.069 for 3680 data with $F_o^2 > 0$. The O–O separation of 1.277 (3) Å and the Co–O–O angle of 120.0 (2)° are consistent with the formal representation of dioxygen coordinated to Co(III) as a superoxide ligand. The axial Co–N(imidazole) and Co–O_2 bond lengths are 2.011 (2) and 1.889 (2) Å, respectively. The imidazole plane and the plane of the Co–O–O grouping are approximately parallel. A comparison of some of the structural parameters of Co(saltmen)(BzlImid)(O_2) with those of two other closely related monomeric dioxygen adducts is given.

Introduction

A wide variety of transition metal complexes which bind one dioxygen ligand per metal atom are now known.[1] The π or symmetrical mode dioxygen bonding is primarily found in complexes of some of the second and third transition series elements; in contrast, σ-bonded dioxygen adducts occur only among some first-row transition metals, primarily iron and cobalt.

The cobalt complex of the Schiff-base ligand 3-MeOsalen was oxygenated in pyridine solution[2] to give the first complex with σ-bonded dioxygen,[3] although it was not definitely characterized because of its low solubility. Other cobalt Schiff-base ligands[4–6] in the presence of a nitrogenous base and the $[Co(CN)_5]^{3-}$ anion in DMF solution[7] have since been shown by x-ray crystallography to bind dioxygen in this manner. The synthesis and the structure determination of a sterically hindered "picket fence" porphyrin[8] have demonstrated the likelihood that this is the mode of dioxygen binding in oxyhemoglobin and oxymyoglobin. Simpler porphyrins of cobalt[9,10] and iron[11] also form 1:1 dioxygen–metal complexes at low temperatures. The evidence for σ-bonded dioxygen in these cases comes primarily from spectral studies.

Our approach to the isolation of σ-bonded dioxygen adducts has been to modify the framework of (*N*,*N*′-ethylene-